ISSN 0016-7029, Geochemistry International, 2006, Vol. 44, No. 10, pp. 1035–1040. © Pleiades Publishing, Inc., 2006.
Original Russian Text © V.A. Kronrod, O.L. Kuskov, 2006, published in Geokhimiya, 2006, No. 10, pp. 1119–1124.

**SHORT COMMUNICATIONS**

# Determining Heat Flows and Radiogenic Heat Generation in the Crust and Lithosphere Based on Seismic Data and Surface Heat Flows

**V. A. Kronrod and O. L. Kuskov**

*Vernadsky Institute of Geochemistry and Analytical Chemistry, Russian Academy of Sciences, ul. Kosygina 19, Moscow, 119991 Russia*

*e-mail: va_kronrod@mail.ru*

Received October 10, 2005

**DOI:** 10.1134/S0016702906100089

The balance of the Earth's energy involves the generation of radiogenic, gravitational, chemical, and other types of energy and the heat loss from the Earth's surface. In the quasi-stationary formulation, heat losses through the surface are equal to the sum of energy generated by all sources in the Earth's interiors. The flow from the continental surface is estimated at 47–49 mW/m$^2$ [1]. Estimates (accomplished by various researchers) of the mantle component of the heat flows range from 3 to 25 mW/m$^2$ [1]. Mantle flows are usually assayed on the basis of extensive geothermal measurements at numerous sites around the world. The heat flow through the Earth's surface $Q_0$ can be expressed as the sum of the mantle flow $Q_M$ and the contribution of radiogenic energy released within the crust $Q_{Cr}$. The value of $Q_{Cr}$ is determined based on geochemical models currently adopted for the distribution of radiogenic elements and the solution of stationary heat conduction [1, 2]. At the same time, the mantle flow $Q_M$ is, in fact, calculated as the difference between $Q_0$ and $Q_{Cr}$. The distribution of K, U, and Th are still known relatively poorly, so that these estimates for both the crust and the mantle broadly differ, and this problem is actively debated in the literature [3, 4].

Thermal models for the mantle are the least definite, mostly because of the uncertainties in the crustal and lithospheric contributions to the overall heat generation [1–4]. The solution to the problem of determining the temperature and/or the chemical composition of the mantle from the velocities of seismic waves was debated in [5–9]. It is quite difficult to derive mantle geotherms from the results obtained by measuring the surface heat flow because of the lack of information on the mantle contribution. This publication proposes a method for assaying the conductive heat transfer of the lithosphere of both mantle and crustal heat flows on the basis of the data of seismic models and the heat flow through the Earth's surface $Q_0$. As an example of such a calculation, we used the profiles of velocities from the IASP91 [10] global reference model (for the "averaged" continental crust) and the BP11A regional model [11], which was developed for the mantle beneath the Kaapvaal craton in South Africa. The solution routine was provisionally subdivided into two stages. During the first of them, the temperature of the mantle ($T_P$ and $T_S$) is determined from the velocities of seismic $P$ and $S$ waves. The procedure of the conversion of seismic profiles into thermal ones is conducted based on the equations of state for the material with regard for anharmonic and anelastic effects. The temperature profile $T_{P,S}$ was then made consistent with the conductive heat transfer model for the crust and mantle, and this enabled us to derive an analytical expression for temperature variations with depth, the values of crustal heat sources, and the components of heat flows in the crust and mantle.

*Determining temperature in the mantle from the velocities of seismic waves.* Geochemical, seismic, and thermal models for the Earth's upper mantle were made mutually consistent using the THERMOSEISM computer program complex and database, by methods of physicochemical simulations, which make it possible to convert compositional models into physical characteristics and velocity profiles into models for the temperature distribution [5, 9, 12, 13]. The temperature $T_P$ in the mantle is determined by solving the inverse problem for the velocities of primary (and/or secondary) seismic waves and the bulk composition of the rock at any point in a depth profile. The equilibrium mineral composition of the rock is determined from the bulk composition by minimizing the Gibbs free energy for the system $Na_2O$–$TiO_2$–CaO–FeO–MgO–$Al_2O_3$–$SiO_2$ with solid solutions of the following minerals: binary solutions of Fe–Mg olivine, spinel, and ilmenite; garnet (*Gar* of the pyrope–almandine–grossular series); orthopyroxene (*Opx*—$MgSiO_3$, $FeSiO_3$, $Ca_{0.5}Mg_{0.5}SiO_3$, $Ca_{0.5}Fe_{0.5}SiO_3$, $Al_2O_3$); and clinopyroxene (*Cpx*—same components plus the jadeite end member) [12, 13]. The

equations of state for the minerals are calculated in the Mie–Grueneiser–Dabye approximation [14]. The constraints assumed for the chemical composition are the depleted material of garnet peridotites and the fertile material of the primitive mantle [15].

The mantle is known to possess dissipative properties, which can be characterized by the mechanical quality factor $Q$. Anelasticity strongly depends on temperature, and its effect should be taken into consideration when seismic velocities at high temperatures are interpreted [16]. Corrections for anelasticity related to seismic attenuation in polycrystalline mantle rocks are assayed by the $Q_S$ and $Q_P$ coefficients.

The two models, which are formally equivalent, for the calculation of $Q_S$ make use of (I) the melting temperature (solidus temperature) and (II) the activation volume [6–8]:

$$\text{model (I)} \quad Q_S(P, T, \omega) = A_1\omega^{\alpha}\exp(\alpha g T_m(P)/T), \quad (1)$$

$$\text{model (II)} \quad Q_S(P, T, \omega) = A_2\omega^{\alpha}\exp(\alpha E^*/RT), \quad E^* = H^* + PV^*, \quad (1a)$$

where $\omega$ is the frequency; $A$, $\alpha$, and $g$ are dimensionless parameters, which insignificantly depend on the frequency; $T_m$ is the solidus temperature; $E^*$, $H^*$, and $V^*$ are the activation energy, enthalpy, and volume; $P$ is the pressure; $R$ is the gas constant; and $T$ is the absolute temperature. The functions $Q_S$ and $Q_P$ are related through

$$Q_P^{-1} = (1 - L)Q_K^{-1} + LQ_S^{-1}, \quad L = 4/3(V_S/V_P)^2. \quad (2)$$

At $Q_K \longrightarrow \infty$, i.e., when the attenuation due to volumetric relaxation can be neglected, the ratio $Q_P/Q_S$ is at a maximum and tends to $1/L$, and $Q_S$ and $Q_P$ are consistent only when $Q_P < Q_S/L$ [17]. With regard for the anharmonic and anelasticity effects, the velocities of $P$ and $S$ waves are related through the expression [6–8]

$$V_{\text{anel}}(P, T, X, \omega) = V_{\text{anh}}(P, T, X)[1 - 1/2Q(P, T, \omega)\tan(\pi\alpha/2)], \quad (3)$$

where the first term in the right-hand part is determined, with correction for anharmony, at a constant composition $X$ by thermodynamic calculations, and the second term characterizes the anelastic absorption of seismic waves and is related to the factor $Q_{S,P}$ by Eqs. (1) and (2). Relations (1–3) enable one to calculate the theoretical velocities of seismic waves and to determine the temperature distribution in the mantle from the experimentally quantified velocities of seismic waves. In this publication, we used model (I). The solidus temperature was specified by the approximating dependence obtained in [18] from experimental data on the solidus temperatures of peridotites within the pressure range of 0–10 GPa.

$$T(^\circ\text{C}) = aP^2 + bP + c, \quad (4)$$

where $a$ = –5.104, $b$ = 132.899, and $c$ = 1120.661, $P$(GPa). The parameters $A$, $\alpha$, $g$, and $E^*$ were estimated in [6–8], in which numerical experiments were reported on the calculation of $Q_S$ at various values of $A$ and $g$ at $\alpha = 0.2$. The values of $A_1$ in the upper mantle were specified within the range of 0.035–1.1 and $g$ within the range of 20–30. An increase in $g$ improves the sensitivity of $Q_S$ to temperature and pressure. The value of $Q_S$ calculated for certain values of $A$ and $g$ should be qualitatively compatible with seismologic models. According to the IASP91 and PREM global seismologic models, the value of $Q_S < 100$ for depths of 100–200 km and $\cong$130–170 for depths of 200–400 km. Based on these data, here we use variable values of the parameter $A_1$ with an exponential dependence on depth to the lower boundary of the lithosphere $H$

$$A_1 = m_1\exp(m_2H/H_{\text{lit}}) \quad (H \le H_{\text{lit}}), \quad A_1 = A_{\text{lit}} \quad (H > H_{\text{lit}}), \quad (5)$$

where the constants $m_1$ and $m_2$ were specified based on the condition of the best correspondence of the temperature profiles calculated according to the IASP91 model to the continental geotherm at a surface flow of 50 mW/m$^2$ [4]: $m_1 = 0.003$ and $m_2 = 6$. The other calculation parameters $Q_S$ had the following values: $\alpha = 0.15$, $g = 30$, $\omega = 0.1$–1. $H_{\text{lit}}$ is the boundary of the thermal lithosphere, which is determined approximately from the transition point from the region with a higher temperature gradient (5–6°C/km) to the region with low gradients, which are close to adiabatic ones. The determination of $H_{\text{lit}}$ usually requires two to three iterations. The calculation results for $Q_S$ by the BPI1A seismological model [11] are portrayed in Fig. 1. $Q_P$ can be calculated if the value of $Q_K$ is known [6, 7]; the values $Q_{K,100} = Q_{K,100\,\text{km}}$ equal to 479 and 1000 were assumed in [6, 7]. However, a constant value for $Q_K$ violates the condition $Q_P/Q_S \longrightarrow 1/L$ at increasing quality factor. Because of this, we assumed a depth-dependent function $Q_K = Q_{K,100}(Q_S/Q_{S,100})^{1.5}$, where $Q_{K,100} = 500$. Our test calculations at $300 < Q_{K,100} < 1000$ have demonstrated that the effect of $Q_{K,100}$ on the calculated temperature does not exceed 20°C at a depth of 100 km.

The temperature distribution with depth $T_{P,S}$ was calculated for a specified seismic profile with corrections for anharmony and anelasticity. At a constant composition, the squared mean deviations of the calculated $V_{\text{anel}}(P, T, X, \omega)$ and experimental seismic velocities are minimized at each depth point by the Newton method. The solution yields a temperature profile with depth and the equilibrium phase composition of the mineral assemblage (phase proportions and their chemical composition) at given $P$–$T$ parameters. The pressure dependence on depth was assumed according to the PREM global model.

*Effect of composition.* To analyze the effect of the mineral composition on the physical characteristics and

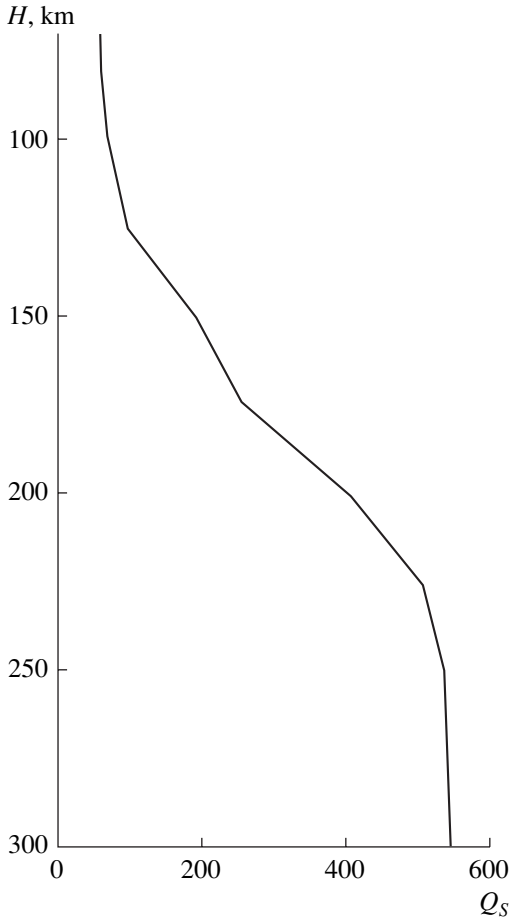


**Fig. 1.** Dependence of the quality factor $Q_S$ on depth $H$ for the BPI1A model [11]. $Q_S$ is determined by Eq. (1), in which the parameter $A_1$ is calculated according to model (5) with an exponential dependence of $A_1$ on depth $H$.

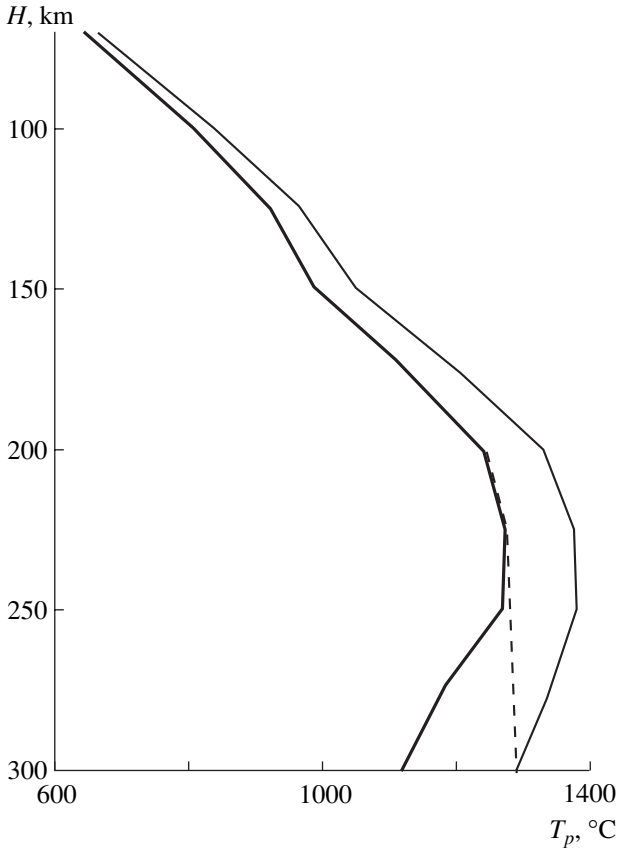


**Fig. 2.** Temperature $T_P$ calculated for the Kaapvaal craton from the $V_P$ profile of the BPI1A model [11]. The heavy line shows the average composition of garnet peridotite (*GP*); the thin line shows the composition of the fertile material of the primitive mantle (*PM*) [15], Table 1; the dashed line corresponds to the composition monotonously changing from *GP* to *PM* at depths of 200–300 km. A temperature inversion occurs at depths of >200 km if the composition does not vary with depth. A variable composition (from GP to PM) at depths of 200–300 km eliminates the temperature inversion.

thermal regime of the upper mantle at depths of 100–300 km, we considered two compositional models (Table 1): (i) a model of the averaged depleted material of garnet peridotites (GP), which was deduced from studying xenoliths in South African kimberlite pipes; and (ii) a model of pyrolite composition, which presumably corresponds to the composition of the fertile material of the primitive mantle (PM) [15]. Figure 2 shows the temperature values calculated by the BPI1A model [11] for all compositions. The temperatures deduced for the GP composition are lower than the temperatures for the PM composition at any depth. At a depth of 300 km, the difference is as significant as 200°C. At a constant composition, a temperature inversion occurs at depths greater than ~200 km. The reasons for this anomaly remain unclear, as yet, and call for further investigation. This feature cannot be caused by the presence of volatiles, fluids, and water-bearing minerals or by partial melting, because any of these factors should have resulted in a decrease, but not increase, of the seismic velocities. Perhaps, the hypothesis of a composition unchanging with depth is inapplicable to the upper mantle. Figure 2 demonstrates that, if the composition is changed from GP to PM, the temperature inversion at depths of 230–300 km can be practically eliminated. Because of this, it is reasonable to expect a change in the chemical composition from the depleted material of the garnet peridotites of Archean cratons (which is depleted in basaltoid components) to fertile primitive-mantle material at depths greater than ~200 km. This hypothesis should be tested.

As also follows from Fig. 2, the temperature boundary layer has an upper boundary in the region with a rapid decrease in the temperature gradient at a depth of ~200 km. If the temperature gradient at depths greater than 220–230 km is close to the adiabatic one, then, at an adiabatic gradient of 0.5°C/km, the temperature at a depth of 400 km should be ~1300°C, which corresponds to a potential adiabat with a surface temperature

**Table 1.** Chemical composition (wt %) of garnet peridotites and the primitive mantle

| Composition, characteristics | Average composition of garnet peridotite | Primitive mantle material |
|---|---|---|
| $SiO_2$ | 45.42 | 45.25 |
| $TiO_2$ | 0.08 | 0.21 |
| $Al_2O_3$ | 1.32 | 4.50 |
| FeO | 7.03 | 8.48 |
| MgO | 45.28 | 37.58 |
| CaO | 0.78 | 3.64 |
| $Na_2O$ | 0.09 | 0.34 |
| Total | 100.0 | 100 |

Note: The compositions of garnet peridotite (GP) and the material of the primitive mantle (PM) are according to McDonough's data [15]. The composition of the phase assemblage was calculated at $P$ = 56.1 kbar and 1250°C. PM composition: 55.6% *Ol* ($Fo_{91}$) + 5.3% *Gar* ($Py_{82}Alm_{14}Gros_4$) + 0.4% *Ilm* ($Geik_{68}$) + 38.7% *Cpx* ($ClEn_{39}Di_{32}ClFs_6Hed_{14}Jd_8ClCor_1$). GP composition: 65.6% *Ol* ($Fo_{92}$) + 1.4% *Gar* ($Py_{85}Alm_{12}Gros_3$) + 0.1% *Ilm* ($Geik_{72}$) + 26.8% *Opx* ($En_{88}OrthoDi_3OrthoFs_{7.3}OrthoHed_{1.2}OrthoCor_{0.5}$) + 6.1% *Cpx* ($ClEn_{42}Di_{27}ClFs_5Hed_{12}Jd_{13}ClCor_1$).

$T_0$ ~ 1100°C. It can be seen in Fig. 2 that the high-velocity South African mantle (BPI1A model) is characterized by low $T_P$ values. These estimates are consistent with geothermal data, according to which the heat flow in the central parts of ancient shields is close to 40 mW/m$^2$ [1–4] and is much higher in the nearby Proterozoic structures. Available data on the heat flow provide no reasons to expect any thermal disturbances within the Kaapvaal craton [19].

*Evaluating heat flows.* The heat transfer from the Earth's surface to the thermal boundary of the lithosphere in a quasistationary regime is usually described by a stationary one-dimensional equation of heat conduction [1, 2]. The thermal boundary of the lithosphere is understood here as the intersection of the calculated temperature profile with the potential adiabat $T_0$ = 1300°C. The heat transfer in our situation is also described within the framework of the stationary model for heat conduction. The whole region of conductive heat transfer (crust + lithosphere) was subdivided into five calculation zones: ($i$ = 1, 2) upper crust, ($i$ = 3) middle crust, ($i$ = 4) lower crust, and ($i$ = 5) lithospheric mantle. Layer $D$ recognized within the upper crust ($i$ = 1) concentrates most sources of radiogenic elements. Radiogenic heat generation *1* in layer $D$ is assumed to be characterized by an exponential distribution with depth $H$: $\theta_1 = \theta_0\exp(-H/D)$ [2], where $\theta_0$ is the generation of radiogenic heat at the surface. The power of sources $i$ in all other zones ($i$ = 2–4) was assumed to be constant within each region. The number of the calculation zones can be decreased, but their overall number must not exceed five. The process of heat transfer is described by the stationary equation of heat conduction

$$\frac{d^2T}{dz^2} = \frac{\theta(z)}{k}, \tag{6}$$

where $z$ is the distance from the upper boundary of each calculation region. The heat thermal conductivity coefficients $k$ were assumed to be constant within each zone [$k = k_i$ ($i$ = 1–5)] [2]. All of the five calculation zones are interrelated through the equality conditions of temperatures and heat flows at common boundaries. At the upper boundary, the temperature $T_0$ and heat flow $q_0$ are specified. An analytical expression for the temperature distribution in each of the calculation zones can be readily deduced from (6). For the upper zone $D$ ($i$ = 1),

$$T_1 = \frac{\theta_1 D^2}{k_1} e^{\frac{-z}{D}} + C_{11}z + C_{12}. \tag{7}$$

The temperature distribution in the other zones ($i$ = 2–5) was determined by the equation

$$T_i = \frac{\theta_i}{2k_i} z^2 + C_{i1}z + C_{i2}. \tag{8}$$

The values of the constants $C_{i1}$ and $C_{i2}$ can be found from the boundary conditions at the surface and between the calculation zones. The boundary conditions at the surface are the temperature and its derivative. The simple dependences (7) and (8) for calculating the temperature for a multilayer model of the crust and lithosphere make it possible to relatively easily solve the inverse problems of heat conduction. The input parameters of the inverse problem involve the thermal conductivity coefficients $k_i$ for all calculation zones, the heat generation in the lower crust $\theta_4$ and lithosphere $\theta_5$, the heat flow at the surface $q_0$, the temperature at the surface $T_0$, and the temperature profile $T_{P,S}$, which is determined from seismic data. The unknown quantities, the thickness of layer $D$, the generation of heat $\theta_1$ in layer $D$, the generation of heat $\theta_2$ in the upper crust at $H > D$, and the generation of heat in the middle crust $\theta_3$, are determined by minimizing the functional $f$ that characterizes the discrepancies between the temperature profile $T_{P,S}$ obtained from seismic data and the temperature $T_K$ calculated by (6–8). To increase the stability of the calculation technique, an additional parameter is introduced that characterizes the overall heat $q_D$ coming from layer $D$. As a result, functional $f$ assumes the form

$$f = \sum_{j=1}^{N} (T_{Kj}^2 - T_{P,Sj}^2) + \delta(q_{DK}^2 - q_a^2), \tag{9}$$

where $N$ is the number of calculation points $j$ in the $T_{P,S}$ profile, and $q_{DK}$ and $q_a$ are the calculated and expected values of $q_D$. The weight coefficient $\delta$ is assumed in such a way that the value of the second term in (9) does

**Table 2.** Heat flows and generation in the crust and lithosphere

| Total heat flow $q_0$, mW/m$^2$ | Mantle heat flow $q_M$, mW/m$^2$; ($q_M/q_0$) | Average heat generation in the crust** $\theta_{crust}$, μW/m$^3$ | Crustal component of $q_0$, $q_{crust}$, mW/m$^2$; ($q_{crust}/q_0$) | Flow $q_D^{***}$, mW/m$^2$ ($q_D/q_0$) | Thickness of layer $D$***, km |
|---|---|---|---|---|---|
| Kaapvaal craton | | | | | |
| 40 | 22 (0.55) | 0.54 (45) | 18 (0.45) | 12 (0.29) | 5.5 |
| 50 | 20 (0.41) | 0.87 (72) | 30 (0.59) | 16 (0.32) | 5.2 |
| Continental mantle | | | | | |
| 48 | 26 (0.53) | 0.55 | 22 (0.47) | 16 (0.33) | 8.4 |
| 52 | 25 (0.47) | 0.67 | 27 (0.53) | 19 (0.36) | 8.2 |
| 55 | 23 (0.42) | 0.77 | 32 (0.58) | 20 (0.36) | 8.1 |

*Heat flow at the lower crust boundary.

**Average heat generation in 35-km-thick crust (values in parentheses are the recalculation to 41-km crust) of the Kaapvaal craton and 41-km-thick continental mantle.

***Heat flow component $q_D$ from the upper layer of thickness $D$ ($q_D = \theta_0 D$) in which the power of heat sources is distributed according to an exponential dependence on depth.

not exceed $0.01f$. Functional $f$ is minimized by the Monte Carlo method. The solution provides all desired parameters and coefficients $C_{i1}$ and $C_{i2}$ ($i$ = 1–5), and this enables the calculation of temperature and heat flows from (7) and (8) for all of the calculation zones.

The following subdivision into calculation zones was assumed for the BPI1A model: upper crust $H <$ 10 km, middle + lower crust 10 km $< H <$ 34 km, and lithosphere $H >$ 35 km. The heat conduction coefficients in all zones and the heat generation in the lithosphere were specified in compliance with the data in [2]. Measurements demonstrate that the average heat flow within the Kaapvaal craton $q_0 \sim 40$ mW/m$^2$ [1–4]. The estimated heat flows in the crust and lithosphere beneath the Kaapvaal craton and in the continental mantle are listed in Table 2.

The average generation of radiogenic heat within the crust of a craton 34 km thick is $\theta_{Cr} = 0.54$ μW/m$^3$ (0.45 μW/m$^3$ when recalculated to a 41-km thickness of the crust) for $q_0 = 40$ mW/m$^2$ and 0.87 μW/m$^3$ for $q_0 =$ 50 mW/m$^2$. The estimates obtained for the Archean crust of South Africa are equal to 0.49–0.78 μW/m$^3$ [2]. The typical average estimates for the generation of radiogenic energy in the Archean crust are 0.48–0.64 μW/m$^3$ [1]. The calculated mantle flow (the flow at the lower lithosphere boundary) of ~20 mW/m$^2$ is consistent with the estimate for the mantle component of the craton heat flow (17 mW/m$^2$). Typical estimates for mantle flows in Archean provinces (these estimates are underlain by various assumptions concerning the distributions of radiogenic elements) lie within the range of 15–21 mW/m$^2$ [1]. The thickness of the thermal lithosphere for a potential temperature of 1300°C is ~220 km. For comparison, the estimated thicknesses of the lithosphere beneath the Kaapvaal craton are as follows: 190–210 km for the thermal models [2], 170–250 km based on the results obtained on xenoliths [2], and up to 300 km based on the results of seismic tomography [21].

The heat flow for the averaged continental crust and lithosphere were determined based on the IASP91 global reference model [10], which is based on a great amount of data on the traveltimes of $P$ and $S$ waves. The results of these calculations are summarized in Table 2. The mantle heat flow for the continental crust was assayed at ~25–26 mW/m$^2$, which corresponds to ~47–53% of $q_0$. According to [2], mantle flows at continents were evaluated for various regions to be equal to 35–62% of $q_0$. The heat flow generated in layer $D$, which is enriched in radiogenic elements, is ~33–36% of $q_0$ (29–40% according to [2]). The average generation of radiogenic sources in the crust is ~0.55–0.77 μW/m$^3$ and lies within the limits of estimates in [1]. The calculated average thickness of the thermal lithosphere beneath continents is ~160–170 km.

**Conclusion.** The method proposed in this publication makes it possible to calculate the thermal regime of the crust and lithosphere (temperatures, heat flows, and heat generation) on the basis of petrological models, data on the velocities of seismic waves, and heat flows at the surface. The good agreement between the results of the model calculations and modern geothermal models for the Kaapvaal craton and continental lithosphere warrant the application of this method as an additional tool for studying heat flows and radiogenic sources in the crust.

## ACKNOWLEDGMENTS

This study was supported by the Russian Foundation for Basic Research (project no. 06-05-64151) and programs of the Division of Earth Sciences of the Russian Academy of Science (Program ONZ-6) and the

Presidium of the Russian Academy of Science (Programs 9 and 18).

## REFERENCES


1. R. L. Rudnick, W. F. McDonough, and R. J. O' Connell, "Thermal Structure, Thickness and Composition of Continental Lithosphere," Chem. Geol. **145**, 395–411 (1998).
2. I. M. Artemieva and W. D. Mooney, "Thermal Thickness and Evolution of Precambrian Lithosphere: A Global Study," J. Geophys. Res. **106**, 16 387–16 414 (2001).
3. R. St. J. Lambert, "Archean Thermal Regimes, Crustal and Upper Mantle Temperatures, and a Progressive Evolutionary Model for the Earth," in *The Early History of the Earth*, Ed. by B. Windley (Wiley, New York, 1976; Mir, Moscow, 1980), pp. 363–376.
4. H. N. Pollack, S. J. Hurter, and J. R. Johnson, "Heat Flow from the Earth's Interior: Analysis of the Global Data Set," Rev. Geophys. **31**, 267–280 (1993).
5. V. A. Kronrod and O. L. Kuskov, "Determination of the Temperature and Bulk Composition of the Upper Mantle from Seismic Data," Geochem. Int. **34**, 72–76 (1996).
6. S. V. Sobolev, H. Zeyen, G. Stoll, et al., "Upper Mantle Temperatures from Teleseismic Tomography of French Massif Central Including Effects of Composition, Mineral Reactions, Anharmonicity, Anelasticity and Partial Melt," Earth Planet. Sci. Lett. **139**, 147–163 (1996).
7. S. Goes, R. Govers, and P. Vacher, "Shallow Mantle Temperatures under Europe from P and S Wave Tomography," J. Geophys. Res. **105**, 11 153–11 169 (2000).
8. F. Cammarano, S. Goes, P. Vacher, and D. Giardini, "Inferring Upper-Mantle Temperatures from Seismic Velocities," Phys. Earth Planet. Inter. **138**, 197–222 (2003).
9. O. L. Kuskov and V. A. Kronrod, "Determination of Mantle Heat Flows Based on Seismic Data," in *Proceedings of 15th Russian Conference on Experimental Mineralogy, Syktyvkar, Russia, 2005* (Syktyvkar, 2005), pp. 60–62 [in Russian].
10. B. L. N. Kennet and E. R. Engdahl, "Traveltimes for Global Earthquake Location and Phase Identification," Geophys. J. Int. **105**, 429–465 (1991).
11. R. E. Simon, C. Wright, E. M. Kgaswane, and M. T. O. Kwadiba, "The P Wavespeed Structure Below and Around the Kaapvaal Craton to Depths of 800 km, from Traveltimes and Waveforms of Local and Regional Earthquakes and Mining-Induced Tremors," Geophys. J. Int. **151**, 132–145 (2002).
12. O. L. Kuskov and V. A. Kronrod, "Core Sizes and Internal Structure of the Earth'S and Jupiter's Satellites," Icarus **151**, 204–227 (2001).
13. O. L. Kuskov and V. A. Kronrod, "Determining the Temperature of the Earth's Continental Upper Mantle from Geochemical and Seismic Data," Geokhimiya, No. 3 (2006) [Geochem. Int. **44**, 232–248 (2006)].
14. O. L. Kuskov and R. F. Galimzyanov, "Thermodynamics of Stable Mineral Assemblages of the Mantle Transition Zone," in *Chem. Phys. Terrestr. Planets*, Ed. by S. K. Saxena (New York, 1986), Vol. 6, pp. 310–361.
15. W. F. McDonough, "Constraints on the Composition of the Continental Lithospheric Mantle," Earth Planet. Sci. Lett. **101**, 1–18 (1990).
16. S. Karato, "Importance of Inelasticity in the Interpretation of Seismic Tomography," Geophys. Rev. Lett. **20**, 1623–1626 (1993).
17. V. N. Zharkov, L. N. Dorofeeva, V. M. Dorofeev, and V. M. Lyubimov, "Test Distribution of Dissipative Function Q(1) in the Earth's Shell," Izv. Akad. Nauk SSSR, Fiz. Zemli **12**, 3–12 (1974).
18. M. M. Hirschmann, "Mantle Solidus: Experimental Constraints and the Effects of Peridotite Composition," Geochem. Geophys. Geosyst. **1**, paper no. 2000GC000070 (2000).
19. M. Q. W. Jones, "Heat Flow in the Witwatersrand Basin and Environs and Its Significance for the South African Shield Geotherm and Lithosphere Thickness," J. Geophys. Res. **93B**, 3243–3260 (1988).
20. C. Jaupart and J.-C. Mareschal, "The Thermal Structure and Thickness of Continental Roots," Lithos **48**, 93–114 (1999).
21. D. E. James, M. J. Fouch, J. C. VanDecar, S. Van Der Lee, and the Kaapvaal Seismic Group, "Tectospheric Structure Beneath Southern Africa," Geophys. Rev. Lett. **28**, 2485–2488 (2001).